occurred. The fact that most metallic meteorites indicate that they were single crystals in the gamma phase (Perry, 1944; Mason, 1962) and have massive phase structures, chemical equilibrium must have been maintained in most metallic meteorites at temperatures above 700°C. Since chemical equilibrium is maintained to 700°C, phosphorus cannot come out of solid solution above the eutectic temperature. The formation of schreibersite by non-equilibrium cooling is therefore highly improbable. Therefore there is only one possible mechanism for the formation of the phosphides observed in the kamacite phase; that is, solid state precipitation.

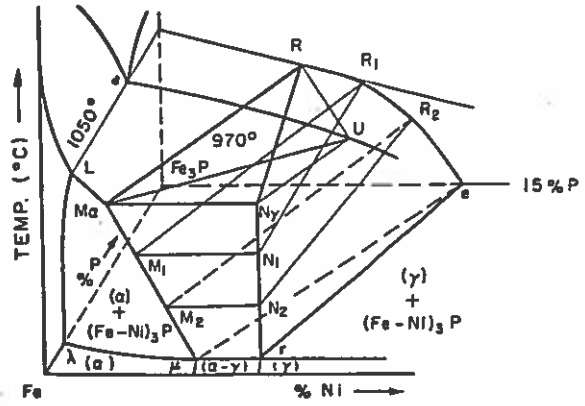

Fig. 8. Fe rich corner of Fe–Ni–P phase diagram.

Phosphides that have eutectic structures were most likely formed by the reheating of the meteorite above the eutectic temperature followed by rapid cooling.

The formation of schreibersite and rhabdite from the solid state can be explained by means of the iron corner of the Fe–Ni–P system. This phase diagram is shown schematically in Fig. 8. U is the composition of the melt at the lowest temperature (970°C) at which it is still in equilibrium with α. At this temperature and at 1 atm pressure there is a non-variant reaction M_α + melt $U \rightleftharpoons N_\gamma + R$, where R is the composition of $(Fe–Ni)_3P$ that forms at this temperature. The compositions at the phase boundaries are not given on the diagram because they are not known to any degree of accuracy. However, the general shape of the ternary diagram (Vogel 1931) is useful in describing the formation of the phosphides.

Hexahedrites have a single phase structure of kamacite (α). When this type of meteorite cools its composition is such that it will pass through the saturation face $\lambda\mu M_\alpha L$ of the α phase and enter the two phase region α + $(Fe–Ni)_3P$, causing the precipitation of phosphides. The temperature at which these precipitates form is determined by the amount of Ni and P in solid solution. When the temperature at which precipitation begins is low, the particles that form are called rhabdites.

In octahedrites, as the temperature of the meteorite decreases, α phase precipitates from γ as it cools below the $(\alpha + \gamma)/\gamma$ surface in the Fe–Ni–P phase diagram. It has been found by electron probe measurements that kamacite has a greater

solubility for phosphorus than taenite. The Grant meteorite has a P content of 0·07 ± 0·01 wt.% in kamacite and 0·025 ± 0·01 wt.% in taenite while the Breece meteorite has a P concentration of 0·075 ± 0·01 wt.% in kamacite and 0·015 ± 0·01 wt.% in taenite. The redistribution of P from γ to α probably occurs even at low temperatures because of the relatively high diffusivity of phosphorus.

As the kamacite grows at the expense of taenite, it also must enrich in nickel. Nickel diffuses from the taenite-kamacite interface into the kamacite and at low temperatures a nickel gradient will be present in the kamacite with a minimum in the center of the band. Therefore it is expected that the center of the kamacite phase will have a lower concentration of nickel than the equilibrium value.

Therefore, upon further cooling the phosphorus content in the nickel poor region of the kamacite exceeds the saturation face $\lambda\mu M_a L$ of the α solid solution and enters the two phase region $\alpha + (Fe\text{–}Ni)_3P$ where schreibersite precipitates. To the best of our knowledge, schreibersite, which is less than 1000 μ in width is always found within the kamacite phase which is in accordance with this theory. Therefore the precipitation of these phosphides cannot begin before the Widmanstätten pattern forms. This process is illustrated in Fig. 9 which shows the Widmanstätten pattern of the Carlton meteorite. After the nucleation of the Widmanstätten platelets, the phosphide particles begin to precipitate and are therefore found in the centers of the fully formed kamacite plates.

According to the Fe–P phase diagram, the solubility of phosphorus in pure iron is 1·0 wt.% at 735°C, 0·25 wt.% at 500°C and 0·015 wt.% at room temperature. The phosphorus content of the Breece and Grant meteorites is 0·57 wt,% and that of the Canyon Diablo meteorite is 0·26 wt.%. Therefore if one assumes that no undercooling occurs before nucleation, phosphide precipitation in the form of schreibersite begins around 650°C in the Grant and Breece and the precipitation of rhabdite at about 500°C in the Canyon Diablo. The effect of Ni is to decrease the solubility of phosphorus in the matrix which will increase the temperature of nucleation slightly.

It can be seen from the Fe–Ni–P phase diagram (Fig. 8) that a phosphide which lies on the same tie-line with a particular composition of kamacite in the $\alpha + (Fe\text{–}Ni)_3P$ two phase field, increases in nickel with decreasing temperature. However, if equilibrium conditions prevail at low temperatures, all the phosphides must have the same compositions no matter what their nucleation temperature was. This condition is not satisfied in meteoric phosphides. It appears that the smaller the size of the precipitates, the higher is the Ni content found in the particles. The data supporting this trend is given in the following table. This data indicates that the largest phosphides have the lowest Ni contents and the rhabdite precipitates have the highest Ni contents. This trend was also found by HENDERSON and PERRY (1958) from examinations of phosphides by chemical analysis. Since the phosphides do not have the equilibrium compositions given by the ternary diagram, a non-equilibrium growth process must have taken place.

After the nucleation of a phosphide particle, the process of growth begins. Evidence that this process occurred is given by the presence of the swathing kamacite region surrounding every phosphide. This is the area through which nickel and phosphorus diffuse from the matrix kamacite to the growing phosphide.

For the phosphides to grow, both phosphorus and nickel must diffuse from

Table 2. Phosphides in the Grant, Breece, and Canyon Diablo Meteorites

Meteorite	Phosphide	Width (μ)	% Ni (average)	% Ni Depletion at Interface	Width of Swathing Kamacite (μ)
Grant (Fig. 4)	Schreibersite	500	23·4	0·9	40
Breece (Fig. 2)	Schreibersite	100	34·8	0·7	25
Breece	Schreibersite	85	36·7	1·0	30
Grant	Schreibersite	75	35·9	1·2	15
Grant (Fig. 5)	Schreibersite	70	37·2	1·4	20
Canyon Diablo (Fig. 7)	Rhabdite	15	43·6	0·8	18
Canyon Diablo	Rhabdite	10	43·9	0·6	10

kamacite into the precipitate. The diffusion coefficient of P in steel is: $D(P, \text{Steel}) = (4{\cdot}5 \times 10^{-2}) \exp(-43{,}000/RT)$ (BARRER, 1951) and the diffusion coefficient of Ni in kamacite is $D(\text{Ni}, \alpha) = 1{\cdot}4 \exp(-58{,}7000/RT)$ (HIRANO *et al.* 1961). The diffusion of phosphorus to the phosphide is much faster than that of Ni. Therefore the diffusion of nickel to the phosphide controls its rate of growth.

With certain simplifying assumptions, one can calculate the growth rate of the phosphides and from this information the probable nucleation temperature and precipitate size. Since the phosphides precipitate below the temperature at which the Widmanstätten pattern begins to form, the phosphides then formed within the approximate temperature range from 750 to 350°C. Within this range the cooling curve for meteoric bodies may be assumed to be linear.

By using Fick's second law and by applying the appropriate boundary conditions for the growth of a planar interface, the phosphide growth distance as a function of time and temperature can be calculated (JOST, 1960). The composition of the kamacite may be expressed by the following equation:

$$C_\alpha = A_\alpha + B_\alpha \operatorname{erf}\left(\frac{x}{2\sqrt{D_\alpha t}}\right) \tag{1}$$

where D_α is the interdiffusion coefficient in the α phase. The movement of the interface (ξ) is a function of time (t) and follows a parabolic law:

$$\xi = 2\gamma\sqrt{D_\alpha t} \tag{2}$$

Figure 10 shows the variation of Ni content as the phosphide grows. The Ni content in kamacite before precipitation is C_α' and the Ni contents at the phosphide-kamacite interface are C' and C''. The initial and boundary conditions are:

at $t = 0, \quad x > 0, \quad C_\alpha = C_\alpha'$

$t > 0, \quad x = \xi, \quad C_\alpha = C'$ (3)

Solving equation (1) using the above conditions (2) and (3)

$$C_\alpha = \frac{C' - C'_\alpha \operatorname{erf}(\gamma)}{1 - \operatorname{erf}(\gamma)} + \frac{C'_\alpha - C'}{1 - \operatorname{erf}(\gamma)} \left(\operatorname{erf} \frac{x}{2\sqrt{D_\alpha t}} \right) \tag{4}$$

γ may be evaluated from a mass balance:

$$(C'' - C') \frac{d\xi}{dt} = D_\alpha \left(\frac{\partial C}{\partial X} \right)_{X>\xi} \tag{5}$$

Differentiating equations (2) and (4) and substituting into equation (5), one obtains the following relation:

$$\sqrt{\pi}\gamma e^{\gamma^2}(1 - \operatorname{erf}(\gamma)) = \frac{C'_\alpha - C'}{C'' - C'} \tag{6}$$

Figure 10 gives a plot of the constant γ versus $(C'_\alpha - C')/(C'' - C')$. Using equation (2) and evaluating γ from Fig. 10, one can calculate the width of the phosphide (2ξ) for any given temperature and time.

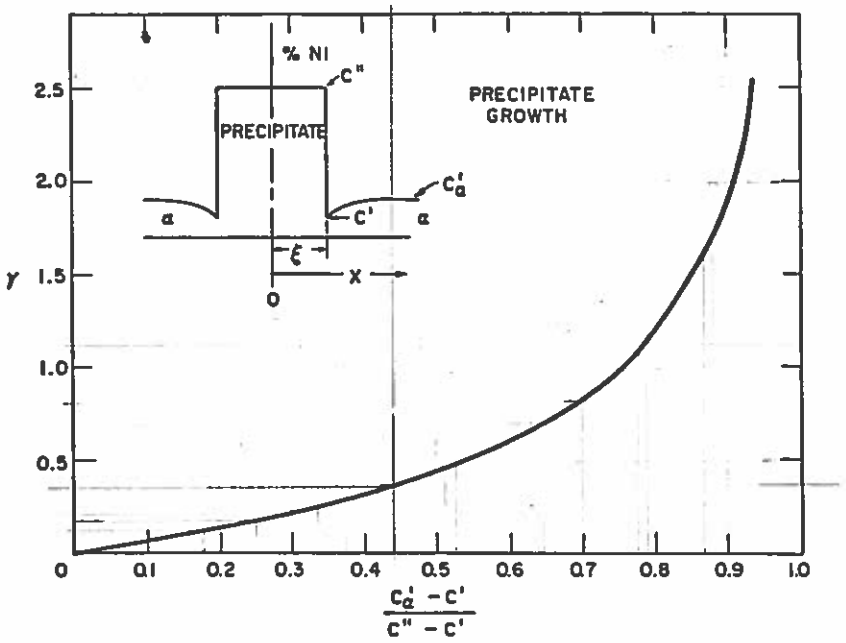

Fig. 10. Schematic of precipitate growth and curve of γ versus the parameter, $C_\alpha' - C'/C'' - C'$.

The conversion from a linear cooling rate S, starting at a given temperature T_0, into an equivalent time at T_0 can be calculated (ARMSTRONG, 1958). The total effect is the same as if the diffusion were carried out at the initial nucleating temperature. The equivalent time is given by:

$$t_{\text{equiv.}} = \frac{RT_0^2}{SQ} \tag{7}$$

where Q is the activation energy for diffusion.